- 1 Hydro-Meteorological Drivers of Event Runoff Characteristics Under Similar Soil
- 2 Moisture Patterns in Three Small-Scale Headwater Catchments
- 3 Adriane Hövel¹, Christine Stumpp¹, Heye Bogena², Andreas Lücke², Peter Strauss³, Günter Blöschl⁴,
- 4 and Michael Stockinger¹
- ¹University of Natural Resources and Life Sciences, Vienna, Department of Water, Atmosphere and
- 6 Environment, Institute of Soil Physics and Rural Water Management, Muthgasse 18, 1190 Vienna,
- 7 Austria
- 8 ²Forschungszentrum Jülich GmbH, Institute of Bio-and Geosciences, Agrosphere Institute (IBG-3),
- 9 Wilhelm-Johnen-Straße, 52425 Jülich, Germany
- ³Institute for Land and Water Management Research, Federal Agency for Water Management,
- Pollnbergstrasse 1, A-3252 Petzenkirchen, Austria
- ⁴Institute of Hydraulic Engineering and Water Resources Management, Vienna University of
- 13 Technology, Karlsplatz 13/223, 1040 Vienna, Austria
- 14 Correspondence to:
- 15 A. Hövel, adriane.hoevel@boku.ac.at

Abstract

16

17

18

19

20

21

22

23

24

25

26

27

28

29

30

31

32

33

34

35

A catchment's runoff response to precipitation largely depends on the antecedent soil moisture, but also on other hydro-meteorological conditions, e.g., evapotranspiration. Studies investigating the effects of hydro-meteorological variables on runoff characteristics in catchments with daily temporal resolution mostly used surrogate measures of soil moisture derived from hydrological models or remote sensing products. Here, we applied a time series-based pattern search to up to 12 years of daily in-situ measured soil moisture in three depths (5, 20, and 50 cm) in three headwater catchments, two of which are located in Germany and one in Austria, to identify key variables influencing runoff characteristics under similar soil moisture patterns. After detecting groups of similar soil moisture, we split the corresponding runoff into similar and different patterns based on goodness-of-fit criteria and analyzed their influencing hydro-meteorological variables with descriptive statistics and Spearman rank correlation coefficients (ρ). Results showed that in the two German catchments, wetness-derived variables, such as the antecedent soil moisture, determined similar runoff patterns under identified soil moisture patterns. In the Austrian catchment, mean groundwater levels influenced different runoff patterns, while rainfall characteristics impacted the normalized peak runoff regardless of the runoff pattern. The proposed method can be used to evaluate hydro-meteorological drivers of event runoff characteristics under similar soil moisture. In this way, hydrological processes that dominate in either group of similar or different runoff patterns can be differentiated, providing insights into the potential predictability of the respective runoff pattern.

Keywords

Catchment hydrology; Runoff characteristics; Patterns; Rainfall-runoff; Soil moisture; Thresholds

1 Introduction

37

38

39

40

41

42

43

44

45

46

47

48

49

50

51

52

53

54

55

56

57

58

59

60

61

62

63

The runoff response to a rainfall event at the catchment scale is driven by climate and physical catchment characteristics (Chen et al., 2020a, 2020b; Jencso & McGlynn, 2011). It is the most comprehensive signature of catchment behavior since it integrates information about different runoff generation processes (Blöschl et al., 2013). Event runoff responses are spatiotemporally variable as they depend on antecedent soil moisture (e.g., Penna et al., 2011; Saffarpour et al., 2016), rainfall characteristics (Blume et al., 2007), and other hydro-meteorological drivers, e.g., evapotranspiration (Guo et al., 2017a; Rossi et al., 2016). Previous studies evaluated runoff generation mechanisms (e.g., Gaál et al., 2012, 2015; Stein et al., 2020; Tarasova et al., 2018a), runoff prediction in ungauged basins (e.g., Parajka et al., 2007), and nutrient transport processes (Grimaldi et al., 2009; James & Roulet, 2007). Thus, exploring drivers of event runoff characteristics contributes to the understanding of catchment-scale hydrological processes and is crucial for informed decision-making not only in water resources management, but also in hydrological modeling (Hrachowitz et al., 2013) and for the development of measurement strategies and their validation (Brocca et al., 2012; Mohanty et al., 2017). However, studies assessing the spatiotemporal dynamics of runoff responses and the factors that drive the fast mobilization of water stored in the catchment for a long time still remain scarce (Kirchner, 2024). Although runoff dynamics were evaluated in single (e.g., Guo et al., 2017b) and multiple catchments with sizes ranging from approx. 5 to 20,000 km² (Gaál et al., 2012; Merz & Blöschl, 2009; Tarasova et al., 2018b; Zheng et al., 2023), only some of them analyzed runoff events based on a large sample of events (e.g., Ali et al., 2010; Tarasova et al., 2018b). At the event scale, respective event characteristics such as the event runoff coefficient (ERC), defined as the ratio of runoff to precipitation, and their driving factors were assessed. Climatic variables, including potential evapotranspiration (PET) and the aridity index, were found to be negatively correlated with ERC, highlighting the role of *PET* in mediating the long-term water storage in soils (Merz & Blöschl, 2009; Rossi et al., 2016; Tarasova et al., 2018b; Zheng et al., 2023). However, Guo et al. (2017b) found in an Australian catchment (27 km²) that rather than climatic variables, daily rainfall intensity had a

large influence on daily runoff. Similarly, ERC were positively correlated with the mean annual precipitation in catchments across Austria (Merz et al., 2006; Merz & Blöschl, 2009) and with event rainfall volumes in large-scale catchments in Germany that had limited storage capacity (Tarasova et al., 2018a). On the contrary, Zheng et al. (2023) found a weak correlation between rainfall volumes and ERC in catchments with large storage capacity, while Rossi et al. (2016) showed that daily rainfall variability was only a secondary driver of daily runoff characteristics. Besides the solely rainfall-derived variables, event runoff variability at the daily scale may be linked to the mean annual or seasonal partitioning of precipitation into evapotranspiration and runoff via soil moisture dynamics (Latron & Gallart, 2008; Rossi et al., 2016). In Austria (Merz & Blöschl, 2009) and the UK (Zheng et al., 2023), ERC and soil moisture followed the same seasonality. In this regard, antecedent soil moisture (ASM) has been shown to strongly influence catchment-scale runoff characteristics (e.g., Penna et al., 2011; Saffarpour et al., 2016). For instance, Singh et al. (2021) investigated soil moisture and runoff responses to rainfall of hillslopes in a headwater catchment and found that ASM and rainfall depth and intensity controlled the relationship between soil moisture and runoff. Furthermore, a nonlinear threshold behavior of the runoff response has frequently been observed in catchments where runoff significantly increased after a certain soil moisture threshold was exceeded (Detty & McGuire, 2010; Jencso et al., 2009; Penna et al., 2011; Stockinger et al., 2014). Despite these advancements, relatively few studies used soil moisture observations at a high spatiotemporal resolution over a long time span to characterize the rainfall-runoff process at the catchment scale (Singh et al., 2021; Vichta et al., 2024). Mostly substitute measures of soil moisture were used, e.g., soil moisture derived from hydrological models or remote sensing products, without discretization of different depths (e.g., Yao et al., 2020; Zheng et al., 2023). Therefore, a better representation of soil moisture is necessary to quantify key influencing variables on the runoff response (Rossi et al., 2016). By clustering similar runoff responses, Hövel et al. (2024a) found that the respective temporal pattern of soil moisture was an important indicator of similar runoff responses. However, they did not investigate temporal patterns in the entire soil moisture time series

64

65

66

67

68

69

70

71

72

73

74

75

76

77

78

79

80

81

82

83

84

85

86

87

88

89

itself, i.e., independent of the times of clustered runoff responses. Examining temporal patterns in both runoff and soil moisture at the same time could help to comprehensively understand catchment-scale rainfall-runoff processes (Blöschl, 2006).

In this study, we addressed this gap by using repeating temporal patterns in soil moisture and runoff at the catchment scale to investigate the interaction between hydro-meteorological variables and event runoff characteristics. To do this, we adopted the approach suggested by Hövel et al. (2024a), but instead of clustering similar runoff responses, we searched for soil moisture patterns averaged over the catchment area in three small-scale catchments providing high resolution *in-situ* soil moisture observations. For each group of similar soil moisture, we divided the respective runoff into similar and different patterns by means of goodness-of-fit criteria to investigate event runoff characteristics and their drivers separately. Therefore, the objectives of the present study were to (1) detect repeating temporal patterns of *in-situ* soil moisture observations, (2) compare the characteristics of similar and different runoff patterns in terms of their major hydro-meteorological drivers, and (3) assess the impact of hydro-meteorological variables on runoff characteristics under similar soil moisture identified in the first objective.

2 Study area and data

2.1 Study sites

Based on their spatiotemporally high-resolution data, we selected three small-scale catchments in

110 Germany and Austria (Figure 1).

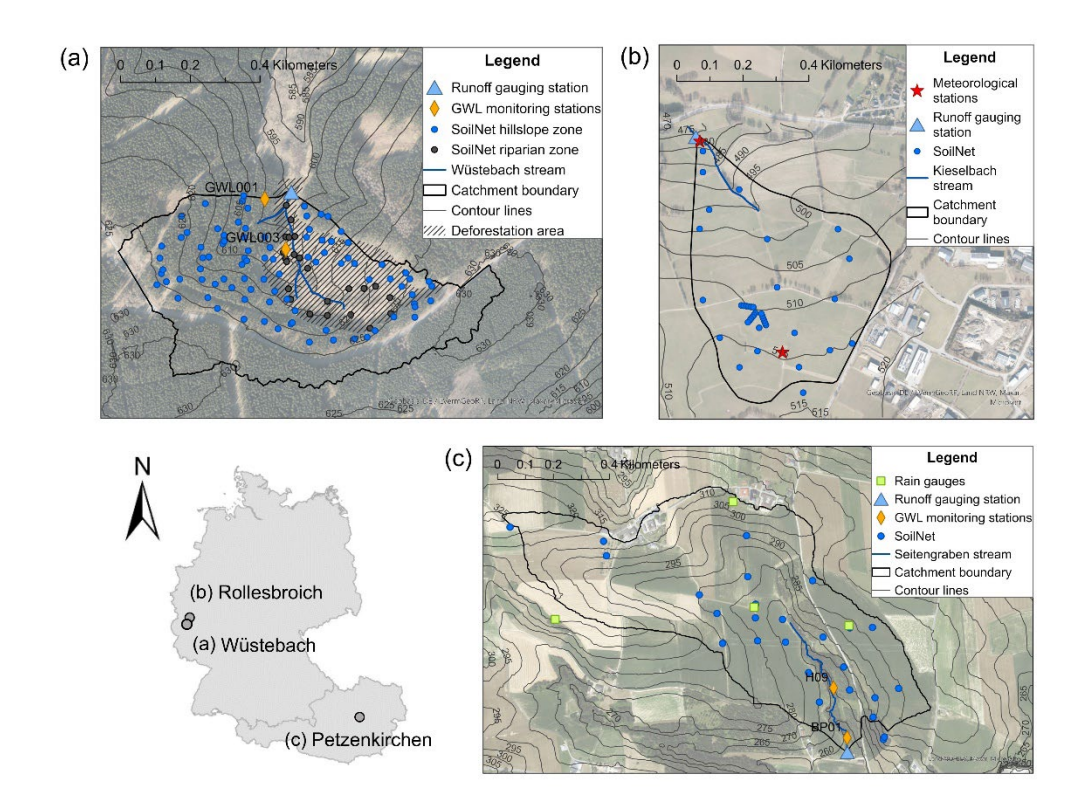


Figure 1. Location and land use maps of the three study catchments in Germany and Austria indicating measurements sites with (a) Wüstebach (partly deforested in 2013), (b) Rollesbroich (extensively managed grassland), and (c) Petzenkirchen (agriculture) (Hövel et al., 2024a).

The Wüstebach (38.5 ha, forest) and Rollesbroich (40 ha, grassland) headwater catchments are located in the Eifel region of western Germany and belong to the Terrestrial Environmental Observatories network (TERENO) (Bogena et al., 2018). Due to their proximity, they are characterized by a similar climate, with a mean annual precipitation of about 1200 and 1033 mm yr⁻¹, mean annual temperature of 7.0 and 7.7°C, and mean annual discharge of about 700 and 520 mm yr⁻¹ in Wüstebach and Rollesbroich, respectively (Zacharias et al., 2011). Soil types of Cambisol and Planosol are predominant in the hillslope zone of the Wüstebach catchment, while the riparian zone (10% of the catchment) is characterized by Gleysols and Histosols. Similarly, gleyic Cambisols prevail further upstream in Rollesbroich, while Stagnosols dominate closer to the outlet (Bogena et al., 2018). Soil depths in the two catchments range from less than 1 m up to a maximum of 2 and 1.5 m in Wüstebach and Rollesbroich, respectively (Gebler et al., 2019; Graf et al., 2014). In Wüstebach,

periglacial layers cover the bedrock (Borchardt, 2012) which consists of Devonian shales and sandstone (Richter, 2008), while in Rollesbroich, the bedrock is covered by weathered saprolite (Gebler et al., 2019). About 21 % (8 ha) of the Wüstebach catchment area, mainly affecting the riparian zone, was deforested in September 2013 (Bogena et al., 2018; Wiekenkamp et al., 2016a). After the clear-cutting, a natural reforestation took place. In Rollesbroich, a drainage system affecting fast runoff processes in the catchment is in the source area (Gebler et al., 2019). The Hydrological Open Air Laboratory (HOAL) Petzenkirchen catchment (66 ha, agriculture) lies in the western part of Lower Austria and has a mean annual precipitation, temperature, and discharge of about 823 mm yr⁻¹, 9.5 °C, and 195 mm yr⁻¹, respectively. The catchment has Gleysols in the riparian zone, while Cambisols and Planosols predominate in most other areas. Soils are shallow and characterized by medium to poor infiltration capacity, with the underlying bedrock consisting of tertiary sediments of the Molasse zone and fractured siltstone (Blöschl et al., 2016). Tile drains are installed in around 15 % of the catchment area and 25 % of the stream is piped, leading to complex, area-specific flow mechanisms (Vreugdenhil et al., 2022).

2.2 Data

- We used high-resolution observation data, including precipitation, runoff, groundwater levels, and *insitu* soil moisture measurements in 5, 20, and 50 cm depth. Figure 2 displays the data for the Wüstebach catchment, while the data for Rollesbroich and Petzenkirchen are shown in Figures S1 and S2 in the Supporting Information, respectively. A detailed description of the data pre-processing and quality control can be found in section 3 "Data and methods" in Hövel et al. (2024a).
- *2.2.1 Precipitation and runoff*
- Daily runoff and precipitation was measured from July 2009 to December 2021 in Wüstebach, from
 January 2010 to October 2022 in Rollesbroich, and from May 2010 to December 2019 in
 Petzenkirchen. In Wüstebach and Rollesbroich, runoff was recorded with a V-notch weir for low
 flows and a Parshall flume for medium to high flows (Bogena et al., 2015; Qu et al., 2016), while in

Petzenkirchen, an H-flume was used (Blöschl et al., 2016). Daily precipitation data for Wüstebach was provided by the Monschau-Kalterherberg meteorological station (DWD, station number 3339). For Rollesbroich, precipitation was acquired from a rain gauge (weighing OTT Pluvio) installed in July 2013 in the center of the catchment and from a Hellmann-type tipping bucket at the outlet from January 2010 to July 2013. Due to low spatial variability between the four available rain gauges (weighing OTT Pluvio) in Petzenkirchen (Vreugdenhil et al., 2022), we calculated daily precipitation as the arithmetic mean of the four gauges.

2.2.2 Soil moisture

153

154

155

156

157

158

159

160

161

162

163

164

165

166

167

168

169

170

171

172

173

174

175

176

177

178

179

Daily soil moisture was available in Wüstebach from July 2009 to December 2021, in Rollesbroich from March 2011 to October 2022, and in Petzenkirchen from July 2013 to December 2019. We used soil moisture data from the SoilNet wireless sensor network installed in Wüstebach in 2009, recorded every 15 min at 5, 20, and 50 cm depth at 150 sites with EC-5 soil moisture sensors (METER Group GmbH, Munich, Germany; Rosenbaum et al., 2012), of which we selected 108 for further analysis based on previous quality controls (Bogena et al., 2010; Wiekenkamp et al., 2016a). In Rollesbroich, soil moisture was measured using a SoilNet equipped with SPADE soil moisture sensors (Qu et al., 2013) from 2011 at 87 sites at the same depths until May 2015. Due to technical problems, the SPADE sensors were replaced by SMT100 soil moisture sensors (Bogena et al., 2017) at 41 SoilNet sites from 2014 onwards, of which we selected 33 stations with continuous data. Data from 2011-2015 was sourced from Qu et al. (2016), and later data from the TERENO data portal (TERENO, 2024). In Petzenkirchen, 32 SoilNet stations equipped with SPADE soil moisture sensors were operated from mid-2013 to late 2021, of which we selected 29 sensors after checking for continuity and outliers. We calculated spatial averages of soil moisture in the three depths over the catchment area in Rollesbroich and Petzenkirchen, while in Wüstebach, we separated the catchment area into a riparian and hillslope zone, as the two zones can be more accurately delineated based on the predominant soil types compared to the other two catchments. Additionally, we calculated a depthweighted mean for a soil depth of 1 m assuming a depth-dependent soil moisture variability in all catchments, with the largest weight of 0.7 given to the measurement in 50 cm, and weights of 0.2 and

0.1 to the measurements in 20 and 5 cm, respectively. Since additional soil moisture measurements in 10 cm in Petzenkirchen were available, we included them into the depth-weighted mean accordingly, with 5 and 10 cm each receiving a weight of 0.05.

2.2.3 Groundwater level

In Wüstebach, we selected two groundwater level measurement sites (Bogena et al., 2015) that showed the best continuity from January 2010 to March 2021. While the station GWL003 is situated upstream near the stream in the deforested zone, GWL001 is further downstream in the forested area (Figure 1). In Petzenkirchen, station H09 recorded groundwater levels from May 2011 to December 2019 and lies in the riparian zone on a lower slope, representing the transition between riparian and hillslope zone (Pavlin et al., 2021; Vreugdenhil et al., 2022). We also selected piezometer BP01 which is situated close to the stream, with data from December 2012 to December 2019 and minimal gaps. Other stations in Petzenkirchen behaved similarly to either H09 or BP01, so that we anticipated the two piezometers to be representative for the catchment. As the groundwater in Rollesbroich is confined and restricted to deep, fractured rocks, no groundwater level observations were available.

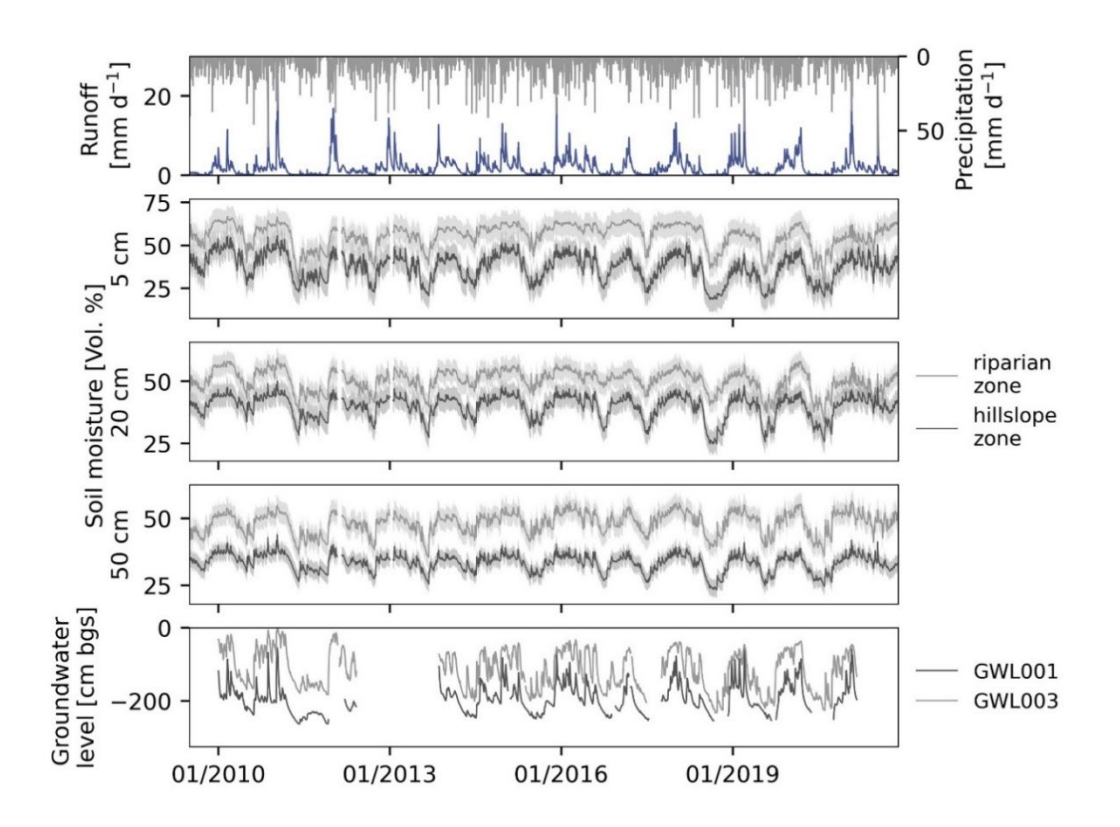


Figure 2. Time series of observed daily precipitation (grey bars from top), runoff at the catchment's outlet (blue), volumetric soil moisture in 5, 20, and 50 cm for the hillslope zone (dark grey) and the riparian zone (light grey), and groundwater level for station GWL 001 (dark grey) and GWL003 (light grey) in the Wüstebach catchment. Grey bands for soil moisture data indicate the spatially-averaged soil moisture value \pm the standard deviation.

3 Methods

3.1 Time series-based soil moisture pattern search

We analyzed the influence of hydro-meteorological variables on event runoff characteristics by implementing a time series-based pattern search in each catchment individually (Figure 3).

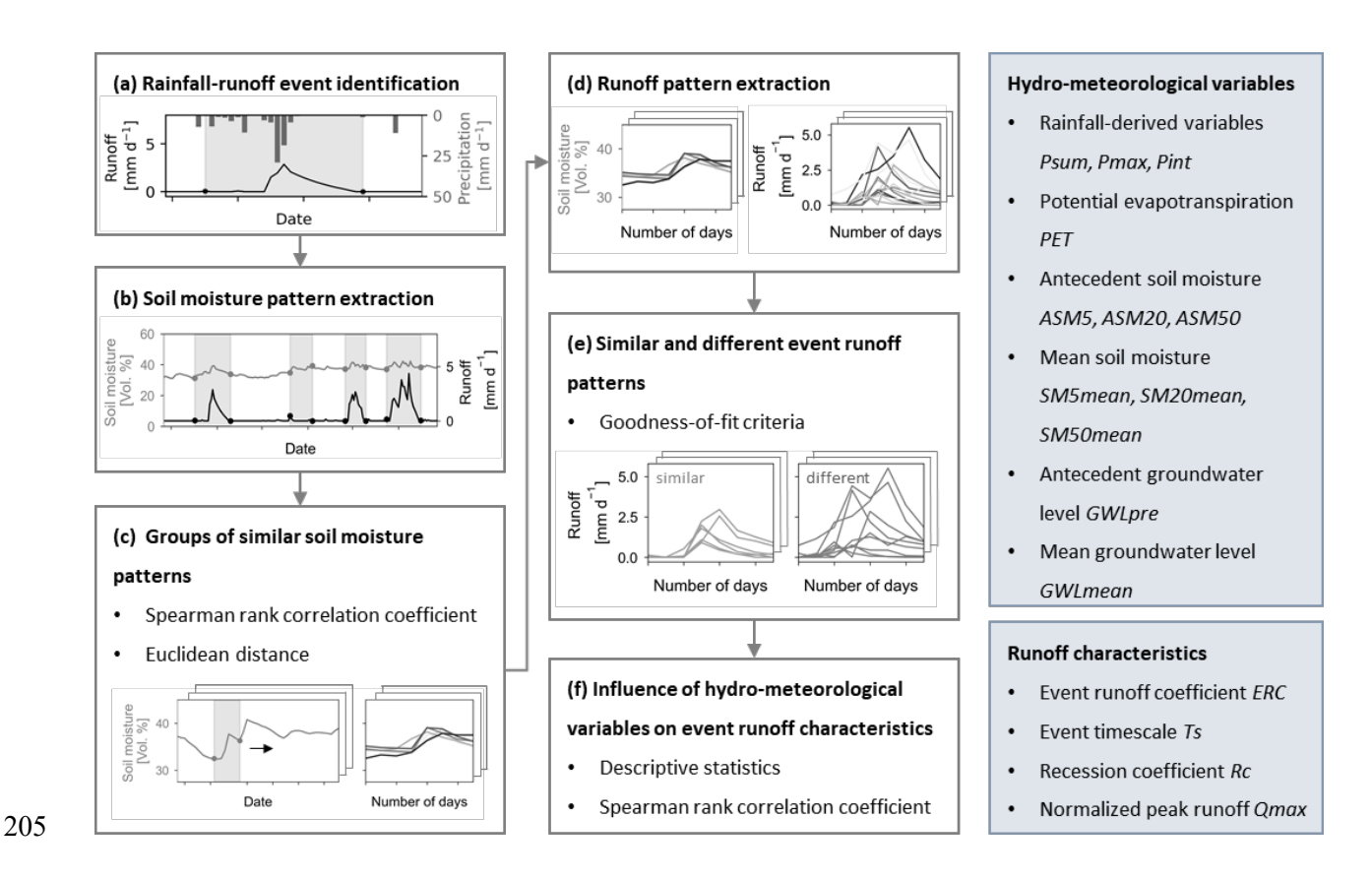


Figure 3. Flow chart of the time series-based pattern search in soil moisture and overview of the runoff characteristics and hydro-meteorological variables used in the analysis.

3.1.1 Runoff event identification

209

210

211

212

213

214

215

216

217

218

219

220

221

222

223

224

225

226

227

228

229

230

231

232

233

234

We identified rainfall-runoff events (Figure 3a) by employing the Detrending Moving-average Cross-correlation Analysis-Event Separation Routine (DMCA-ESR; Giani et al., (2022)). The method does not require subjective parameter choices and has been successfully applied in other catchment-scale studies (e.g., Zheng et al., 2023). Further, it does not require an *a priori* base flow separation; the base flow component is separated after identification for each event by taking the minimum runoff before the rising limb (Giani et al., 2022). We excluded events falling below the mean runoff, which has been adopted by previous studies as a meaningful threshold for runoff event identification (e.g., Hövel et al., 2024a; Zheng et al., 2023).

3.1.2 Similarity of soil moisture and runoff patterns

For each runoff event, we extracted the concurrent depth-weighted mean soil moisture (Figure 3b) and used it to find similar soil moisture patterns at different times in the same catchment (Figure 3c). For this, we applied the Matrix Profile method which was developed to robustly identify all patterns that match a specific pattern in the time series (Madrid et al., 2019; Yeh et al., 2016). Trivial matches such as very close ones ($\pm 25\%$ of the pattern length) are automatically excluded, significantly reducing the computation time. For patterns to match, pre-defined similarity criteria had to be met. We defined two criteria to assess the similarity of soil moisture patterns: (1) they exceeded a Spearman rank correlation coefficient threshold of 0.76, 0.74, and 0.53 in Wüstebach, Rollesbroich, and Petzenkirchen, respectively (adapted from Hövel et al., 2024a), and (2) the Euclidean distance between them was lower than 5 Vol. % to account for absolute deviations between patterns. The correlation coefficient thresholds represent the mean correlation between soil moisture patterns of similar runoff events (Hövel et al., 2024a) and were therefore used as a threshold. Consequently, groups of similar soil moisture patterns were derived. Since the groups were based on the depthweighted mean soil moisture, we additionally assessed the relationship between soil moisture patterns in the three measurement depths of 5, 20, and 50 cm by calculating the Pearson correlation coefficient (r) and evaluating its significance on a 95% confidence level (p < 0.05).

For each group of similar soil moisture patterns, we divided the respective runoff into similar and different patterns based on goodness-of-fit criteria (Figure 3e). We combined the Nash-Sutcliffe-Efficiency (NSE, Eq. 1), with a volume error (VE, Eq. 2) to form the Nash-Volume Error (NVE) as suggested by Lindström (1997):

$$NSE = 1 - \frac{\sum_{i=1}^{n} (Q_1 - Q_2)^2}{\sum_{i=1}^{n} (\bar{Q}_2 - Q_2)^2}$$
 (1)

$$VE = \frac{\sum_{i=1}^{n} |Q_1 - Q_2|}{\sum_{i=1}^{n} Q_2}$$
 (2)

$$NVE = NSE - \chi |VE| \tag{3}$$

 Q_1 and Q_2 represent the respective runoff events identified, with \bar{Q} denoting the mean over the event duration (n days). The parameter χ serves as a weighting factor for the volume error set to 0.1 according to Lindström (1997). We defined events to be similar if the Nash-Volume Error (NVE) exceeded a threshold of 0.65 (Moriasi et al., 2007; Saleh et al., 2000; Singh et al., 2005). In the subsequent analysis, we focused only on groups of soil moisture patterns for which both similar and different runoff patterns could be identified.

3.2 Runoff characteristics

For all runoff patterns, we assessed four descriptive characteristics (Table 1): The event runoff coefficient (ERC), the peak runoff normalized by the long-term mean runoff (Qmax), the ratio of runoff volume to peak runoff (Ts), and the recession coefficient (Rc). The latter was derived from event-based recession analysis, which characterizes the nonlinear decrease in runoff after a peak over time, typically described by a power law differential equation (Brutsaert & Nieber, 1977):

$$\frac{\mathrm{d}Q}{\mathrm{d}t} = -aQ^b \tag{4a}$$

$$Q(t) = (Q_0^{1-b} - (1-b)at)^{\frac{1}{1-b}}$$
(4b)

 $\frac{dQ}{dt}$ is the rate of change in runoff Q, Q_0 is the runoff at the start of the recession segment, t is the length of the recession segment, and a and b are the recession model parameters.

In contrast to classical recession analysis, which aims at a single parametrization of the recession model, the event-based analysis enables assessing variations in the catchment's runoff response over time with respect to e.g., different wetness states (Biswal & Nagesh Kumar, 2014; Patnaik et al., 2015). Previous studies showed that nonlinear fitting to absolute values of the recession segment produces reliable estimates of recession scale parameter a and exponent b (Chen & Krajewski, 2016; Dralle et al., 2015, 2017; Wittenberg & Sivapalan, 1999), so that we applied nonlinear fitting.

Because reliable comparison of recession coefficients between events is only possible for the exponent b (Berghuijs et al., 2016a; Dralle et al., 2017), we used b as the recession coefficient (Rc) in our analysis. We calculated the four runoff characteristics for each runoff pattern individually and then averaged them over each group of similar soil moisture patterns (Figure 3d). Furthermore, we calculated mean runoff characteristics of similar and different runoff patterns separately, and indicated the coefficient of variation (CV) for all respective mean characteristics.

Table 1. Event runoff characteristics used as target variables.

Variable	Abbreviation	Definition	Equation	References
Event runoff coefficient	ERC [-]	Ratio of the event runoff volume [mm] to the event rainfall volume [mm]	$ERC = \frac{Q_{vol}}{P_{vol}}$	Merz et al., 2006; Sherman, 1932
Event timescale	Ts [days]	Ratio of event runoff volume [mm] to the peak runoff [mm d ⁻¹]	$Ts = \frac{Q_{vol}}{Q_{peak}}$	Gaál et al., 2012
Recession coefficient	Rc [-]	Exponent <i>b</i> in the power law recession model	$\frac{\mathrm{d}Q}{\mathrm{d}t} = -aQ^b$	Brutsaert & Nieber, 1977; Dralle et al., 2015, 2017
Normalized peak runoff	Qmax [-]	Maximum event runoff [mm d ⁻¹] normalized by the long-term mean runoff [mm d ⁻¹]	$Q_{max} = \frac{Q_{peak}}{\overline{Q}}$	Tarasova et al., 2018b

3.3 Hydro-meteorological variables

Rainfall-derived variables included the event rainfall sum Psum [mm], the maximum event rainfall intensity Pmax [mm d⁻¹], and the event mean rainfall intensity Pint [mm d⁻¹]. Furthermore, we calculated the event mean potential evapotranspiration PET [mm d⁻¹] with the Penman-Monteith equation. In terms of wetness-derived variables, we assessed the impact of antecedent soil moisture one day before the event ASM5, ASM20, ASM50 [Vol. %] and the event mean soil moisture SM5mean, SM20mean, SM50mean [Vol. %] in measurement depths of 5, 20, and 50 cm, respectively. Additionally, we calculated the groundwater level one day before the event GWLpre [cm bgs] and the event mean groundwater level GWLmean [cm bgs] in Wüstebach and Petzenkirchen. Groundwater level measurement gaps at the daily scale amounted to approx. 15 % and 4 % at stations GWL001 and GWL003 in Wüstebach, respectively, and 6 % and 5 % at stations H09 and BP01 in Petzenkirchen, respectively. We allocated meteorological seasons of spring (March, April, May), summer (June, July, August), autumn (September, October, November), and winter (December, January, and February) to all patterns based on their day of occurrence. To analyze how hydro-meteorological variables influenced the runoff patterns in respective seasons, we used the Spearman rank correlation coefficient (ρ) and evaluated its significance based on a 95 % confidence level (p < 0.05).

4 Results

4.1 Time series-based soil moisture pattern search

A total of 100, 95, and 120 runoff events and concurrent soil moisture patterns (Figure 3b) were extracted in Wüstebach, Rollesbroich, and Petzenkirchen, respectively. Only considering soil moisture patterns for which similar and different runoff patterns were identified (Figure 3e), 62, 16, and 55 groups of similar soil moisture patterns were formed in Wüstebach, Rollesbroich, and Petzenkirchen, respectively. Within each group, we detected the highest number of soil moisture patterns in Wüstebach, followed by Petzenkirchen and Rollesbroich. Particularly in Wüstebach, we observed a high average number of matches for one soil moisture pattern (Table S1 in Supporting

Information). Thus, soil moisture patterns were not restricted to times when runoff events were identified but were distributed across the entire time series. While in the two German catchments, most groups consisted of wetting and subsequent drying patterns, soil moisture patterns in Petzenkirchen mainly comprised wetting-up patterns with higher variability within one group than in the other catchments, as shown by the broad confidence intervals (Figure S3 in Supporting Information). In Rollesbroich, we particularly observed consistent wetting-up and drying patterns of soil moisture with one distinct peak for most groups (Figure 4). Although in Wüstebach, most groups showed a similar pattern to Rollesbroich, there were also patterns with slower drying after the peak compared to the rest of the groups (Figure S4 in Supporting Information).

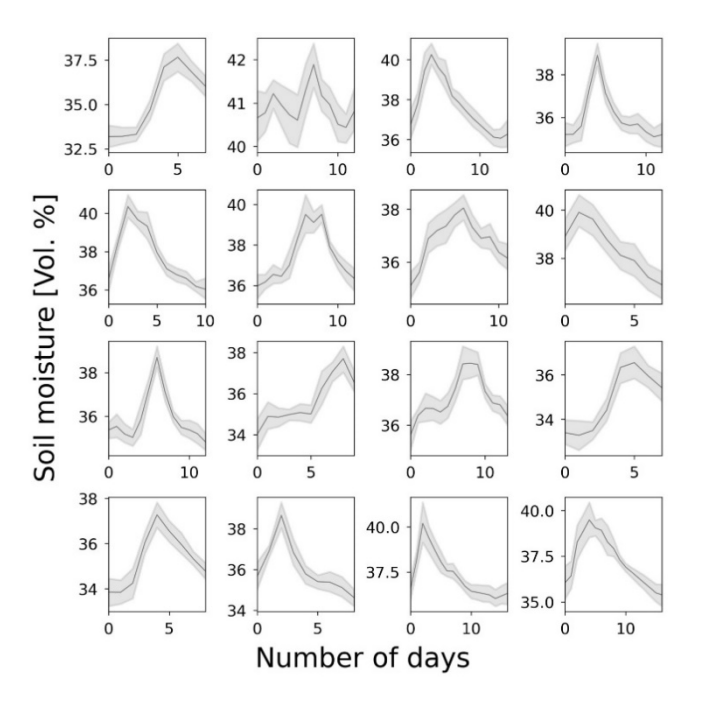


Figure 4. Groups of similar soil moisture patterns in the Rollesbroich catchment, indicating the mean soil moisture in each group and the corresponding 95% confidence interval.

Regarding the different soil moisture measurement depths for the identified patterns, we found a strong significant correlation between the soil moisture in 5 cm and 20 cm depth in Wüstebach (r =

0.83) and Petzenkirchen (r = 0.72), but not in Rollesbroich (r = 0.31). While correlation coefficients remained low between soil moisture in 5 cm and 50 cm in Rollesbroich and Petzenkirchen (Figure S5 in Supporting Information), soil moisture in the two layers was significantly correlated in Wüstebach at 0.61. The percentages of the runoff patterns attributed to either the group of similar or different runoff for each group of similar soil moisture patterns differed between the catchments. In Petzenkirchen, the average number of similar runoff patterns for one soil moisture pattern was higher than the number of different patterns, in contrast to the other two catchments (Table S1 in Supporting Information).

4.2 Runoff characteristics and their seasonality

Wüstebach and Rollesbroich had overall comparable runoff characteristics under similar soil moisture patterns, particularly in terms of mean event runoff coefficients *ERC* (0.25 and 0.27, respectively) and timescales *Ts* (5.08 and 4.42 days, respectively) (Table 2). In contrast, Petzenkirchen showed lower mean *ERC* and shorter *Ts* compared to the other two catchments with 0.09 and 2.38 days, respectively, with *ERC* having the largest coefficient of variation (CV) of all runoff characteristics in the catchment at 0.73. In Wüstebach, we observed the highest CV for the recession coefficient *Rc* with 1.20, while in Rollesbroich, CV was largest for the normalized peak runoff *Qmax* at 0.80 (Table 2).

Table 2. Descriptive statistics of runoff characteristics averaged over all runoff patterns in the respective groups of similar soil moisture patterns detected in the three catchments, including their mean and coefficient of variation (CV).

		Wüstebach	Rollesbroich	Petzenkirchen
ERC [-]	Mean	0.25	0.27	0.09
	CV	0.88	0.72	0.73

Ts [days]	Mean	5.08	4.42	2.38
	CV	0.49	0.46	0.32
Rc [-]	Mean	0.75	0.98	1.02
	CV	1.20	0.76	0.41
Qmax [-]	Mean	4.71	6.37	18.61
	CV	1.08	0.80	0.56

The runoff characteristics in the three catchments varied throughout the year: Event runoff coefficients *ERC* in Wüstebach and Petzenkirchen followed a seasonal pattern, also for the differentiation between similar and different runoff patterns, with *ERC* being highest in winter and lowest in summer (Figure 5). In contrast, *ERC* in Rollesbroich varied considerably between the two groups of runoff patterns in spring.

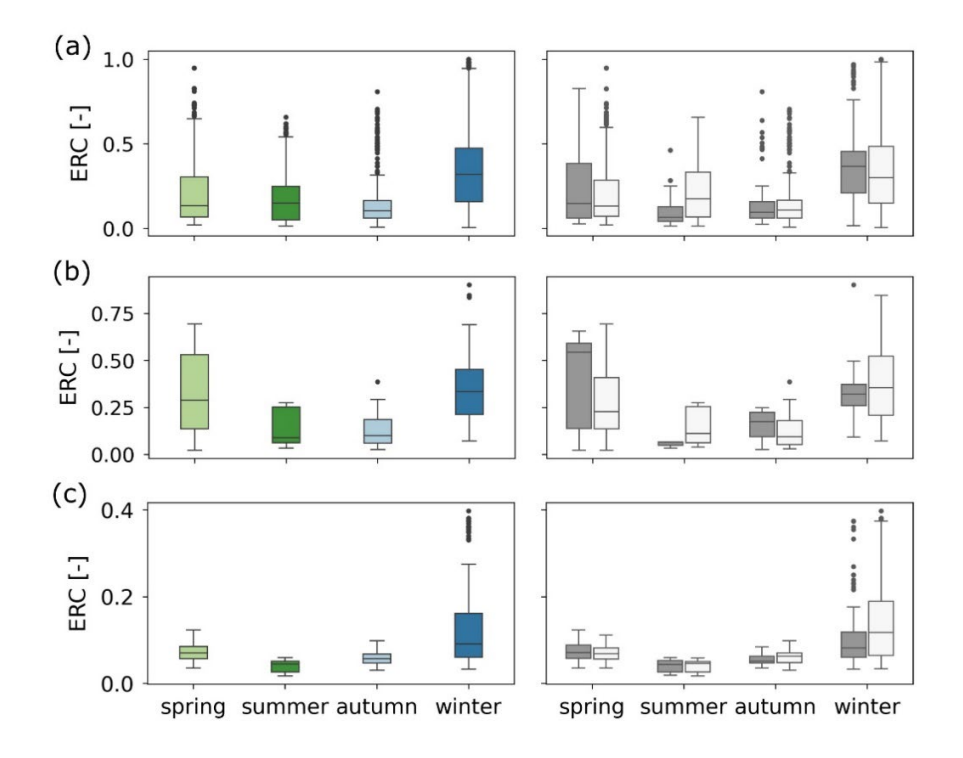


Figure 5. Event runoff coefficients *ERC* for spring, summer, autumn, and winter, including all runoff patterns in the left column and separated between similar (grey) and different (light grey) runoff patterns in the right column for (a) Wüstebach, (b) Rollesbroich, and (c) Petzenkirchen.

Ts in Wüstebach and Rollesbroich followed the same seasonality as ERC, with longer Ts in spring and winter compared to the rest of the year (Figure S6 in Supporting Information). In Rollesbroich, the same seasonality was also evident for Qmax (Figure S7 in Supporting Information). In contrast, Ts in Petzenkirchen showed no major seasonal variations (CV=0.32) and was, on average, shorter (\sim 2 days) than in Wüstebach (\sim 5 days) and Rollesbroich (\sim 4.5 days). Similarly, we did not detect a distinct seasonal pattern of the recession coefficient Rc in Petzenkirchen. On average, we found the largest Rc in Petzenkirchen in winter, whereas in Wüstebach and Rollesbroich, Rc were highest in the summer (Figure S8 in Supporting Information). In all three catchments, we generally observed shorter Ts and lower Rc for similar runoff patterns compared to different ones. Furthermore, the variability of Qmax was lower in the group of similar runoff patterns than in the group of different patterns in all catchments. This was particularly evident in Rollesbroich, with a CV of 0.51 and 0.86, respectively.

4.3 Linking hydro-meteorological variables and their seasonal dynamics with runoff

characteristics

4.3.1 Similar runoff patterns

For similar runoff patterns, all runoff characteristics were, on average, mostly significantly correlated with wetness-derived variables in Wüstebach (ASM50, SM50mean, and GWLmean) and Rollesbroich (ASM5 and SM5mean), while in Petzenkirchen only ERC and Rc were primarily correlated with these. Figure 6 displays the Spearman rank correlation coefficients (ρ) between runoff characteristics and hydro-meteorological variables in Wüstebach, differentiated between similar and different runoff (Figures S9 and S10 for Rollesbroich and Petzenkirchen, respectively, in Supporting Information).

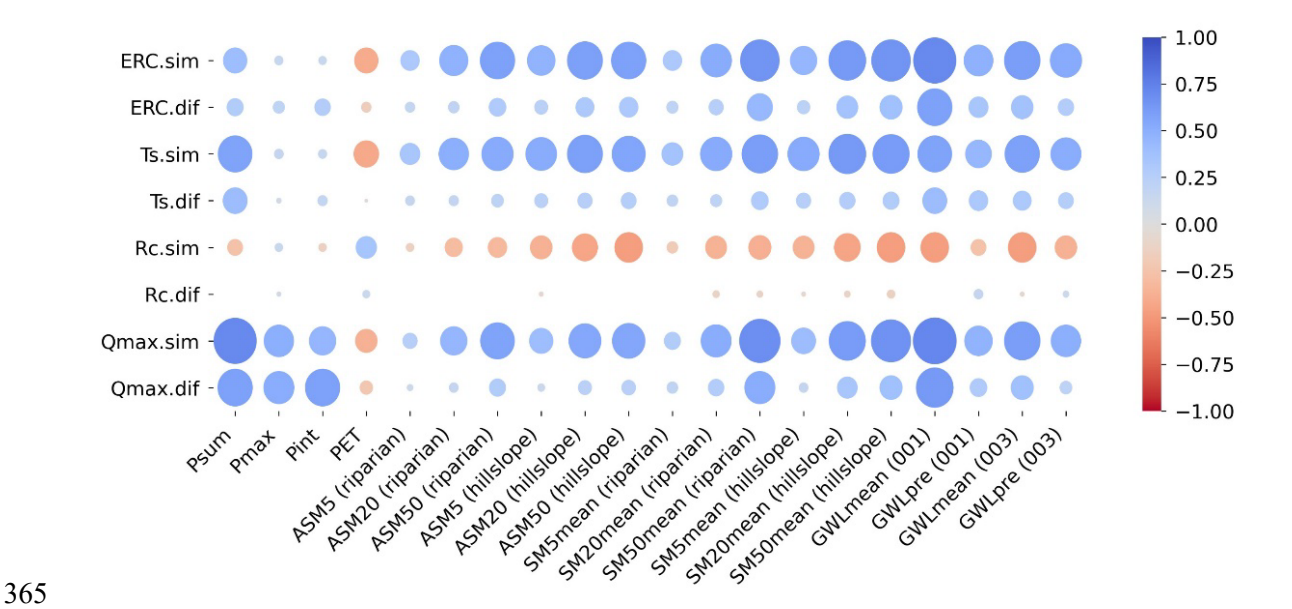


Figure 6. Heatmap showing Spearman rank correlation coefficients (ρ) between event runoff characteristics and selected hydro-meteorological variables (p < 0.05), separated between groups of similar (e.g., *ERC.sim*) and different (e.g., *ERC.dif*) runoff patterns in the Wüstebach catchment. The size and color of the dots both indicate the value of the correlation coefficient for better visualization.

ERC was significantly correlated with ASM in 50 cm in both the riparian ($\rho=0.58$) and hillslope ($\rho=0.58$) zone in Wüstebach and in Petzenkirchen ($\rho=0.56$). In comparison, in Rollesbroich it was correlated with ASM in 5 cm ($\rho=0.52$). In all catchments, we observed a threshold relationship of ERC with ASM in the respective depths, with ERC and ASM being seasonally related for similar runoff patterns: Soil moisture in summer rarely reached a threshold after which ERC substantially increased, so that ERC generally remained low. In contrast, the largest ranges of ERC with values from 0 to 1 occurred in winter (Figure 7). The thresholds in ASM were approx. 48 and 33 Vol. % in 50 cm soil depth in the riparian and hillslope zone of Wüstebach, respectively, and 48 and 38 Vol. % in 5 and 50 cm in Rollesbroich and Petzenkirchen, respectively (Figure 7).

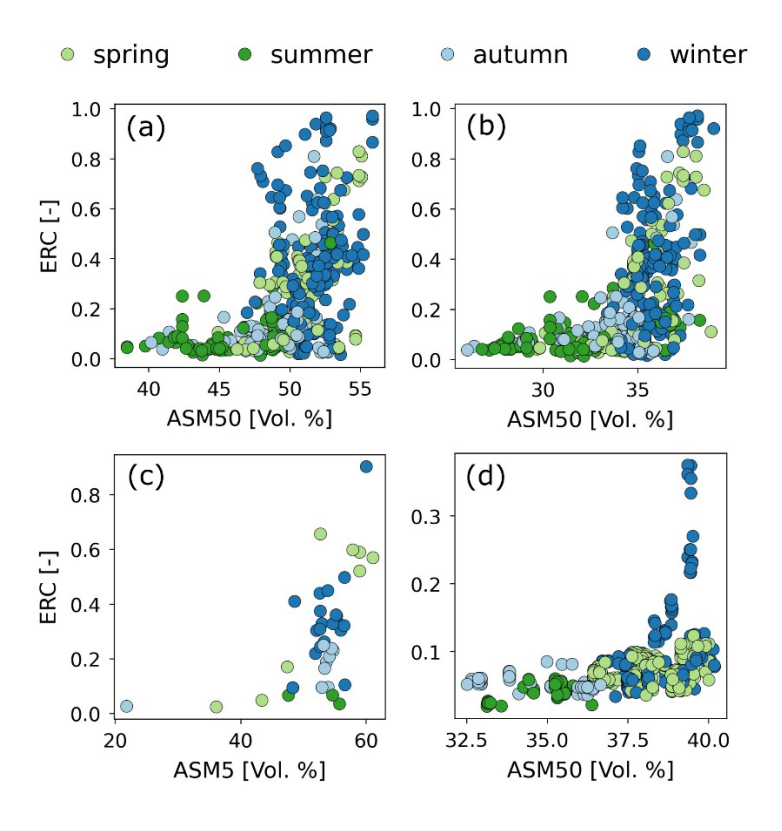


Figure 7. Relationship between antecedent soil moisture *ASM* and event runoff coefficient *ERC* in (a) the riparian zone and (b) hillslope zone of the Wüstebach catchment in 50 cm (*ASM50*), (c) in the Rollesbroich catchment in 5 cm (*ASM5*) and (d) in the Petzenkirchen catchment in 50 cm (*ASM50*), for similar runoff patterns.

In addition to ASM, we found a significant correlation between ERC and mean event groundwater levels (GWLmean) at both piezometers in Wüstebach ($\rho=0.71$ and $\rho=0.60$ at GWL001 and GWL003, respectively). Similarly, ERC and GWLmean at H09 and BP01 were significantly correlated in Petzenkirchen ($\rho=0.39$ and $\rho=0.59$, respectively) with seasonal differences of higher groundwater levels and ERC in the winter season compared to the other seasons (Figure S11 in Supporting Information). Furthermore, the nonlinearity of recession, Rc, had the highest correlations with wetness-derived variables compared to the other hydro-meteorological variables in all three catchments for similar runoff patterns. In Wüstebach and Rollesbroich, soil moisture in 50 cm had a major influence on Rc, with a significant correlation between Rc and antecedent and mean soil moisture in the hillslope zone in Wüstebach ($\rho=-0.47$), and mean soil moisture in Rollesbroich ($\rho=-0.47$), and mean soil moisture in Rollesbroich ($\rho=-0.47$), and mean soil moisture in Rollesbroich ($\rho=-0.47$).

0.44) in the respective depth. In addition, Rc was correlated with GWLmean at both piezometers in Wüstebach ($\rho = -0.47$) and in Petzenkirchen with mean and pre-event GWL at piezometer H09. While we identified rainfall-derived variables as the sole drivers of Qmax in Petzenkirchen, correlation coefficients between Ts and hydro-meteorological variables were generally low for similar runoff patterns in the catchment (Figure S10 in Supporting Information). Conversely, groundwater levels and ASM in deep layers had an additional impact on Qmax and Ts in Wüstebach. In Rollesbroich, mean soil moisture in 5 cm was the most important factor influencing the two runoff characteristics, with a significant correlation coefficient of 0.59.

4.3.2 Different runoff patterns

396

397

398

399

400

401

402

403

404

405

406

407

408

409

410

411

412

413

414

415

416

417

418

419

420

421

422

In Wüstebach and Rollesbroich, correlation coefficients were in most cases lower in the group of different runoff patterns compared to the similar ones. If not, differences were marginal (e.g., $\rho = 0.15$ and $\rho = 0.20$ between ERC and Pmax in Wüstebach for similar and different runoff patterns, respectively). Meanwhile, influencing factors for *Qmax* shifted from wetness-derived to rainfallderived variables in both catchments (Figure 6 and Figure S9 in Supporting Information): We found a significant positive correlation between *Qmax* and rainfall volumes *Psum* and intensities *Pint* for different runoff patterns, with values of 0.58 and 0.56 for Psum and 0.58 and 0.53 for Pint in Wüstebach and Rollesbroich, respectively. Furthermore, the threshold relationship between ERC and ASM observed in both catchments was not as pronounced for different runoff patterns (Figure S12 in Supporting Information) as for similar patterns. For instance, we observed an increased ERC of 0.6 also for low ASM in the hillslope zone (ASM50 around 33 Vol. %) in the Wüstebach catchment. On the contrary, Petzenkirchen also showed a pronounced threshold relationship between ERC and ASM50 for different runoff patterns (Figure S12 in Supporting Information). In general, we found higher correlation coefficients for different rather than similar runoff patterns more frequently in Petzenkirchen than in the other two catchments. This was particularly evident for the runoff characteristics of ERC, Rc, and Qmax: Correlation coefficients were stronger between ERC and groundwater levels in Petzenkirchen for different runoff patterns compared to similar ones. Likewise, we observed higher correlations between Rc and wetness-derived variables for different runoff

patterns than similar ones, with mean and antecedent soil moisture in 20 cm having the highest correlation with Rc ($\rho = 0.54$). In addition to rainfall-derived variables being significantly correlated with Qmax, wetness-derived variables showed increased correlations with Qmax for different runoff patterns compared to similar ones in Petzenkirchen (Figure S10 in Supporting Information). In contrast, in the two German catchments, particularly in Rollesbroich, wetness-derived variables did not show any significant correlation with Qmax for different runoff patterns.

429

430

431

432

433

434

435

436

437

438

439

440

441

442

443

444

445

446

447

448

423

424

425

426

427

428

5 Discussion

5.1 Temporal patterns in soil moisture and their linkage to respective runoff

patterns

We showed that different soil moisture patterns extracted based on runoff events were recurrent over time in the catchments studied. Since we conducted the pattern search over the entire time series based on the pre-defined similarity criteria, soil moisture patterns were additionally identified independently of runoff events. Therefore, we detected similar soil moisture patterns also during dry conditions, because not only rainfall-driven wetting but also radiation-driven drying influences soil moisture dynamics (Liu et al., 2024; Mälicke et al., 2020). We found the largest number of similar soil moisture patterns in Wüstebach, indicating low variability and therefore high recurrence of the wetting and subsequent drying cycles in soil moisture. Although soil moisture patterns in Rollesbroich showed similar wetting-up and drying cycles (Figure 4), comparatively few repeating soil moisture patterns were found in the catchment. As soil moisture patterns in 5 cm were not well correlated with those in 20 cm (r = 0.31) or 50 cm depth (r = 0.39), the large weights of both 20 cm and 50 cm soil moisture in the depth-weighted mean might have resulted in fewer recurrent soil moisture patterns in Rollesbroich. In contrast to the other two catchments, patterns of similar soil moisture in Petzenkirchen were more variable, as indicated by the broad confidence intervals within the groups (Figure S3 in Supporting Information). The large variability of soil moisture patterns within one group may also result from the comparably low correlation coefficient we set as a similarity criterion for the

soil moisture patterns to match in Petzenkirchen ($\rho = 0.53$). Most patterns did not follow a clear wetting and drying, but rather a continuous wetting-up, with the soil moisture peak following the runoff peak (Figure S3 in Supporting Information), as also reported by Pavlin et al. (2021) for Petzenkirchen.

As for the respective runoff patterns, the majority of runoff under similar soil moisture patterns in the German catchments was classified as different (Table S1 in Supporting Information), showing that runoff patterns were variable over time. In contrast, in Petzenkirchen, although similar soil moisture patterns showed high variability, the group of similar runoff was on average larger than the one of different patterns. This suggests an increased number of similar runoff patterns in the catchment compared to Wüstebach and Rollesbroich, as also indicated by the high number of clusters containing similar runoff events (Hövel et al., 2024a). Even though runoff mechanisms in different sub-parts of the Petzenkirchen catchment are complex, as shown by Vreugdenhil et al. (2022), our study demonstrates that the catchment average runoff response at the outlet shows a high degree of repeatability over time.

5.2 Differentiation between similar and different runoff patterns under similar soil moisture patterns

In the catchments studied, we observed a change in major driving factors of runoff characteristics from similar to different runoff patterns. While similar runoff patterns were predominantly influenced by wetness-derived variables in Wüstebach and Rollesbroich, the normalized peak runoff of different patterns was mainly controlled by rainfall volumes and intensities. Previous studies suggested that intensity-driven, i.e., rainfall-driven, runoff responses may be associated with infiltration excess flow mechanisms, while storage-driven responses may result from saturation excess mechanisms (Ali et al., 2015; McDonnell, 2013; McGrath et al., 2007). In Wüstebach and Rollesbroich, saturation excess flow may thus only be attributed to similar runoff patterns, which are mainly driven by storage-driven, i.e., wetness-derived, variables. In contrast to the German catchments, differing between influencing

variables of similar and different runoff patterns under similar soil moisture in Petzenkirchen was more complex. We found that correlation coefficients between hydro-meteorological variables and runoff characteristics were more often higher for different runoff patterns than for similar ones, suggesting that the underlying temporal soil moisture pattern was not the dominant factor in defining the runoff response pattern in the catchment, as also reported by Hövel et al. (2024a). While both rainfall- and wetness-derived variables impacted characteristics of similar runoff patterns, mean groundwater levels became even more important in the group of different compared to similar runoff patterns. The key role of groundwater-derived variables for different runoff patterns implies that the water stored in groundwater bodies and corresponding hydraulic conductivities determined the overall shape of the hydrograph at the outlet in Petzenkirchen.

5.3 Hydro-meteorological drivers of event runoff characteristics and their linkage to

catchment wetness states

5.3.1 Influence of rainfall-derived variables on runoff characteristics

Rainfall characteristics, particularly *Psum* and *Pint* mainly impacted runoff characteristics of *ERC*, *Ts*, and *Qmax* in the catchments studied. In Wüstebach and Rollesbroich, especially *Qmax* for different runoff patterns showed a significant positive correlation with *Psum* and *Pint*. A strong positive correlation between rainfall volumes and *Qmax* was also found by Tarasova et al. (2018b), possibly hinting at a wet catchment state leading to an increase of event runoff coefficients *ERC* (Berghuijs et al., 2016b). Conversely, we observed a significant negative correlation between rainfall and *ERC* in Petzenkirchen, where even low *Psum* led to high *ERC*, which were triggered by long, consistent, low-intensity rainfall events in winter times (Figure S13 in Supporting Information). This somewhat counterintuitive observation is supported by the findings of Merz & Blöschl (2009) in other Austrian catchments, for which low maximum rainfall intensities also led to high event runoff coefficients. They attributed this phenomenon to the rainfall characteristics in Austria, with rainfall events of longer duration leading to higher runoff coefficients than shorter, more intensive rainfall events.

Furthermore, *Psum* and *Pint* equally impacted *Qmax* of similar and different runoff patterns in Petzenkirchen, indicating a significant influence of the two rainfall characteristics on the normalized peak runoff regardless of the observed hydrograph shape. Still, similar shapes of the runoff response at the catchment's outlet were also found to be influenced by the temporal pattern of incoming precipitation (Hövel et al., 2024a). The dominant control of rainfall characteristics on the runoff response in Petzenkirchen is further supported by Szeles et al. (2024), who found a high contribution of new water (~50 %) during peak flows, suggesting a rapid contribution of precipitation to the stream via surface runoff. Surface runoff in the catchment may occur for various reasons, with agricultural land use and soil compaction being one of the major influencing factors (Szeles et al., 2024).

5.3.2 Influence of wetness-derived variables on runoff characteristics

501

502

503

504

505

506

507

508

509

510

511

512

513

514

515

516

517

518

519

520

521

522

523

524

525

526

527

In Wüstebach, soil moisture in 50 cm and mean groundwater level (GWLmean) at GWL001 strongly influenced runoff characteristics of similar runoff patterns. We observed higher correlations between GWLmean at GWL001 and ERC and Qmax compared to GWL003. This is consistent with the results of Hövel et al. (2024a), who found that groundwater levels at GWL001 showed higher correlations for similar runoff responses compared to GWL003. The discrepancy between the two sites may be due to station GWL003 being influenced by the deforestation in September 2013 in the catchment, while GWL001 remained undisturbed. Furthermore, the strong impact of ASM in deep soil layers may be explained by macro pores allowing deeper infiltration in forest soils compared to e.g., grasslands (e.g., Alaoui et al., 2011). Thus, precipitation reaching deeper soil layers might have contributed to the catchment's runoff as subsurface stormflow. Wiekenkamp et al. (2016b) observed catchment-wide preferential flow during both relatively dry and extremely wet conditions in Wüstebach. Similar results have been reported by Vichta et al. (2024) in a forested headwater catchment, highlighting the role of trees in transporting water to deeper soil layers via preferential flow paths. Our results in Wüstebach, therefore, suggest an overall fast pressure response between soil moisture, groundwater level, and the stream due to potentially high hydraulic conductivity and preferential flow paths in the subsurface, resulting in similar runoff patterns at the catchment's outlet. Isotope data analyzed in the catchment further support this observation, where streamflow was found to substantially consist of

groundwater, and the young water fraction (fraction of water younger than 3 months) was generally low at approx. 10 % (Stockinger et al., 2019). Furthermore, runoff generation often depends on a threshold in ASM (e.g., Detty & McGuire, 2010; Tromp-Van Meerveld & McDonnell, 2006). Threshold relationships between ASM and runoff have been observed in previous studies (e.g., Jeneso et al., 2009; Penna et al., 2011); also for Wüstebach, where the hillslope zone is known to contribute to runoff above a soil moisture threshold when subsurface connectivity is established (Stockinger et al., 2014). Based on the high number of matches for one soil moisture pattern in Wüstebach, an increase in ERC was only apparent after a certain soil moisture threshold was reached (Figure 7). Therefore, soil moisture patterns that remained below this threshold did not trigger a corresponding runoff event detected by the event identification method, indicating significant subsurface storage capacity in the catchment. This storage capacity is confirmed by model results of Hrachowitz et al. (2021) in the Wüstebach catchment; they suggest a storage volume of at least ~8000 mm in the layered and fractured Devonian shale bedrock. However, the high storage capacity may also be due to the subsurface being connected to surrounding areas outside the boundaries of the surface catchment area. In contrast to Wüstebach, the dominant role of ASM in the Rollesbroich grassland catchment in the topsoil rather than the deep layer may be due to increased bulk density and reduced infiltration of water down to deeper layers (Alaoui et al., 2011; Li & Shao, 2006). Qu et al. (2016) showed that bulk density increased with soil depth based on 273 soil samples in Rollesbroich. The strong correlations we observed between mean soil moisture in 5 cm and ERC, Ts, and Qmax might therefore be due to fast interflow close to the surface resulting from higher hydraulic conductivity in the upper soil layer compared to the deeper layers. In Petzenkirchen, we found the threshold relationship between ERC and ASM in 50 cm to hold for both similar and different runoff patterns, indicating that this relationship controlled ERC of all runoff patterns in the catchment. Still, ERC and Omax for different runoff patterns may additionally be influenced by water bypassing the soil or preferential flow through the installed tile drains in the catchment. In terms of seasonality, small rainfall sums combined with high ASM leading to high ERC

528

529

530

531

532

533

534

535

536

537

538

539

540

541

542

543

544

545

546

547

548

549

550

551

552

553

also hint at a consistent subsurface connectivity during wet winter months in Petzenkirchen, as also indicated by Széles et al. (2018) and Vreugdenhil et al. (2022). However, the catchment's overall shorter Ts and therefore flashier response (2.4 days) compared to the other two catchments indicates a decreased available subsurface soil storage capacity due to shallow soils with medium to poor infiltration capacities (Blöschl et al., 2016; Gaál et al., 2012; Vreugdenhil et al., 2022). In addition, the earlier response of the stream compared to the soil moisture in the catchment might indicate overland flow processes, i.e., a faster connection of overland flow paths to the stream compared to the subsurface (e.g., Beiter et al., 2020). The significant correlations between *Omax* and *Pint* for both similar and different runoff patterns further support the presence of infiltration excess overland flow. Furthermore, we found significant correlations between runoff characteristics, particularly ERC, and *GWLmean* at H09 and BP01 ($\rho = 0.69$ and $\rho = 0.65$, respectively) in Petzenkirchen for different runoff patterns, suggesting that groundwater contributes to the stream most times of the year (Eder et al., 2022; Exner-Kittridge et al., 2016). Although Pavlin et al. (2021) proposed a continuous connection of the riparian zone to the stream, our results showed that pre-event groundwater levels at BP01 may have a limited impact on runoff characteristics with a low mean correlation coefficient of 0.23. We therefore assume that it is not the absolute pre-event groundwater level, but the prevalent subsurface properties, which influence the groundwater level over time, that may determine the shape of the hydrograph. The recession coefficient Rc and ASM in 20 cm in Petzenkirchen were significantly correlated for different runoff patterns ($\rho = 0.54$). The nonlinearity in recession increased from dry to wet catchment states, i.e., when riparian-hillslope connectivity was reached, which was also found in mountainous catchments (Harman et al., 2009; Lee et al., 2023). However, in Wüstebach and Rollesbroich, we observed the opposite relationship with a significant negative correlation between Rc and ASM in 50 cm for similar runoff patterns, i.e., increased nonlinearity of the recession in dry conditions. Saffarpour et al. (2016) also suggested that recession is slower the wetter the catchment, and vice versa, leading to the observed shorter timescale during dry conditions, which was additionally found by Latron & Gallart (2008). Furthermore, Gaál et al. (2012) suggested that a short timescale in dry

555

556

557

558

559

560

561

562

563

564

565

566

567

568

569

570

571

572

573

574

575

576

577

578

579

580

conditions may be due to more efficient drainage compared to wet catchment conditions, even for high rainfall sums. The increased recession nonlinearity and shorter timescales in Wüstebach in dry conditions may additionally be amplified by evapotranspiration effects ($\rho = 0.35$). Since Rc was mainly influenced by wetness-derived variables in all three catchments, subsurface properties, especially hydraulic conductivity, may have a strong influence on recession behavior. In this regard, Biswal & Marani (2010) investigated basins across the US and also found geomorphological features of the sites to mainly control recession curves. In our study, the diverging findings between the catchments in terms of Rc and Ts and their major drivers could also be attributed to site-specific geomorphological properties, requiring a more detailed investigation in further studies.

5.4 Limitations and possible future applications

In the past, most studies analyzing catchment-scale temporal patterns either focused on soil moisture without considering respective event runoff characteristics (Korres et al., 2015; Liu et al., 2024; Mälicke et al., 2020; Rosenbaum et al., 2012) or investigated patterns only in runoff (e.g., Gaál et al., 2016). Here, we directly linked runoff and soil moisture through the pattern search, with the soil moisture patterns based on the times when runoff events were identified. Similarly, Araki et al. (2022) linked soil moisture to runoff and suggested that particularly event-based soil moisture signatures, e.g., the event rise time, could potentially provide inference about the dominant runoff response type (Araki et al., 2022). In our study, dividing corresponding runoff patterns into similar and different ones under similar soil moisture provided insights into the recurrence of runoff patterns and their hydro-meteorological drivers. Classifying runoff responses may thus also allow conclusions to be drawn about the predictability of the respective runoff pattern. In this regard, Zehe et al. (2007) highlighted that runoff predictability was mainly influenced by an interplay of the initial state of the system and threshold dynamics, which is in line with our observations in the catchments analyzed. However, our approach also has some limitations. Since the pattern search was based on depthweighted mean soil moisture, with the largest weight assigned to the deep soil layer, short-term dynamics in the topsoil may have been improperly accounted for. Furthermore, the similarity of soil

moisture patterns was based on correlation coefficient thresholds derived by Hövel et al. (2024a), and it needs to be tested in the future whether different thresholds would lead to different results. The time series-based pattern search could also be expanded to other catchments with a large variety of physical and climatic conditions where soil moisture data is available to evaluate influencing factors on event runoff characteristics. In this way, the method may be used to distinguish between runoff processes dominating in groups of similar and different runoff patterns based on a large sample of catchments.

616

617

618

619

620

621

622

623

624

625

626

627

628

629

630

631

632

633

634

635

609

610

611

612

613

614

615

6 Summary and conclusions

We detected repeating temporal patterns in soil moisture and analyzed the influence of hydrometeorological variables on the corresponding runoff characteristics. Repeating soil moisture patterns occurred in all three catchments studied, with more groups of similar patterns formed in Wüstebach and Petzenkirchen compared to Rollesbroich. Splitting respective runoff patterns into similar and different, we found that while the wetness-derived variables of antecedent soil moisture and groundwater levels were significantly correlated with event characteristics for similar runoff patterns, correlation coefficients mainly decreased for different runoff patterns in the two German catchments. Our results, therefore, demonstrated that wetness-derived variables were decisive for generating a similar runoff response during similar soil moisture conditions in two of three catchments tested. In Wüstebach, the strong influence of soil moisture and groundwater levels implied a fast pressure response between the wetness-derived variables and the stream. In Rollesbroich, the dominant role of soil moisture in the topsoil suggested a substantial contribution of interflow to the stream. In the Austrian catchment, runoff characteristics of similar runoff patterns showed a stronger correlation with rainfall-derived variables in addition to soil moisture. At the same time, mean groundwater levels mainly influenced different runoff patterns. Furthermore, rainfall characteristics impacted the normalized peak runoff, irrespective of the shape of the observed hydrograph. Together with the observed earlier peak of the hydrograph compared to soil moisture for identified patterns, our results emphasize the importance of overland flow processes in the catchment.

While our method could differentiate between influencing factors of similar and different runoff patterns in the German catchments, major drivers of runoff characteristics varied for respective patterns in the Austrian catchment. The time series-based pattern search thus provides a novel framework for analyzing runoff characteristics and their drivers, helping to evaluate the dominant hydrological processes in small-scale catchments. Extending the proposed approach to a large sample of catchments has the potential to improve our understanding of the recurrence and thus the possible predictability of runoff patterns and their drivers.

Acknowledgements

This work was funded by the Austrian Science Fund (FWF – Österreichischer Wissenschaftsfonds) [grant number 10.55776/P34666]. We acknowledge the support by TERENO (Terrestrial Environmental Observatories) of the Helmholtz Association of National Research Centers (HGF), Germany. The work of Adriane Hövel was supported by the Doctoral School "Human River Systems in the 21st Century (HR21)" of the University of Natural Resources and Life Sciences, Vienna. We also thank the Austrian Federal Agency for Water Management for providing the data for the Petzenkirchen catchment.

Data Availability Statement

The time series data necessary to reproduce the findings of the study are available in the following data repository: https://doi.org/10.5281/zenodo.13753239 (Hövel et al., 2024b). Furthermore, the tool for the runoff event identification (Giani et al., 2022) used in this paper is available at https://github.com/giuliagiani/DMCA-ESR. The *stumpy* library (Python) including the Matrix Profile algorithm (Yeh et al., 2016) used for the time series-based pattern search can be accessed under https://stumpy.readthedocs.io/en/latest/install.html.

661 Conflict of Interest

The authors declare no conflict of interest relevant to this study.

References

663

687

Alaoui, A., Caduff, U., Gerke, H. H., & Weingartner, R. (2011). Preferential Flow Effects on 664 665 Infiltration and Runoff in Grassland and Forest Soils. Vadose Zone Journal, 10(1), 367–377. 666 https://doi.org/10.2136/vzj2010.0076 667 Ali, G., Roy, A., Turmel, M. C., & Courchesne, F. (2010). Multivariate analysis as a tool to infer 668 hydrologic response types and controlling variables in a humid temperate catchment. Hydrological Processes, 24(20), 2912–2923. https://doi.org/10.1002/hyp.7705 669 Ali, G., Tetzlaff, D., McDonnell, J. J., Soulsby, C., Carey, S., Laudon, H., Mcguire, K., Buttle, J., 670 671 Seibert, J., & Shanley, J. (2015). Comparison of threshold hydrologic response across northern 672 catchments. Hydrological Processes, 29(16), 3575–3591. https://doi.org/10.1002/hyp.10527 673 Araki, R., Branger, F., Wiekenkamp, I., & McMillan, H. (2022). A signature-based approach to 674 quantify soil moisture dynamics under contrasting land-uses. Hydrological Processes, 36(4), 1– 21. https://doi.org/10.1002/hyp.14553 675 Beiter, D., Weiler, M., & Blume, T. (2020). Characterising hillslope-stream connectivity with a joint 676 677 event analysis of stream and groundwater levels. Hydrology and Earth System Sciences, 24(12), 678 5713-5744. https://doi.org/10.5194/hess-24-5713-2020 679 Berghuijs, W. R., Hartmann, A., & Woods, R. A. (2016a). Streamflow sensitivity to water storage changes across Europe. Geophysical Research Letters, 43(5), 1980–1987. 680 https://doi.org/10.1002/2016GL067927 681 682 Berghuijs, W. R., Woods, R. A., Hutton, C. J., & Sivapalan, M. (2016b). Dominant flood generating 683 mechanisms across the United States. Geophysical Research Letters, 43(9), 4382–4390. 684 https://doi.org/10.1002/2016GL068070 685 Biswal, B., & Marani, M. (2010). Geomorphological origin of recession curves. Geophysical Research Letters, 37(24), 1-5. https://doi.org/10.1029/2010GL045415 686

Biswal, B., & Nagesh Kumar, D. (2014). Study of dynamic behaviour of recession curves.

- 688 *Hydrological Processes*, 28(3), 784–792. https://doi.org/10.1002/hyp.9604
- Blöschl, G. (2006). Hydrologic synthesis: Across processes, places, and scales. Water Resources
- 690 Research, 42(3), 2–4. https://doi.org/10.1029/2005WR004319
- Blöschl, G., Blaschke, A. P., Broer, M., Bucher, C., Carr, G., Chen, X., Eder, A., Exner-Kittridge, M.,
- Farnleitner, A., Flores-Orozco, A., Haas, P., Hogan, P., Kazemi Amiri, A., Oismüller, M.,
- Parajka, J., Silasari, R., Stadler, P., Strauss, P., Vreugdenhil, M., ... Zessner, M. (2016). The
- Hydrological Open Air Laboratory (HOAL) in Petzenkirchen: A hypothesis-driven observatory.
- 695 *Hydrology and Earth System Sciences*, 20(1), 227–255. https://doi.org/10.5194/hess-20-227-
- 696 2016
- 697 Blöschl, G., Sivapalan, M., Wagener, T., Viglione, A., Savenije, H., & (Eds.). (2013). Runoff
- 698 Prediction in Ungauged Basins Synthesis across Processes, Places and Scales. Cambridge
- 699 University Press.
- Blume, T., Zehe, E., & Bronstert, A. (2007). Rainfall-runoff response, event-based runoff coefficients
- and hydrograph separation. *Hydrological Sciences Journal*, *52*(5), 843–862.
- 702 https://doi.org/10.1623/hysj.52.5.843
- Bogena, H. R., Bol, R., Borchard, N., Brüggemann, N., Diekkrüger, B., Drüe, C., Groh, J., Gottselig,
- N., Huisman, J. A., Lücke, A., Missong, A., Neuwirth, B., Pütz, T., Schmidt, M., Stockinger,
- M., Tappe, W., Weihermüller, L., Wiekenkamp, I., & Vereecken, H. (2015). A terrestrial
- observatory approach to the integrated investigation of the effects of deforestation on water,
- energy, and matter fluxes. Science China Earth Sciences, 58(1), 61–75.
- 708 https://doi.org/10.1007/s11430-014-4911-7
- Bogena, H. R., Herbst, M., Huisman, J. A., Rosenbaum, U., Weuthen, A., & Vereecken, H. (2010).
- 710 Potential of Wireless Sensor Networks for Measuring Soil Water Content Variability. *Vadose*
- 711 Zone Journal, 9(4), 1002–1013. https://doi.org/10.2136/vzj2009.0173
- Bogena, H. R., Huisman, J. A., Schilling, B., Weuthen, A., & Vereecken, H. (2017). Effective

713 calibration of low-cost soil water content sensors. Sensors, 17(1), 208. 714 https://doi.org/10.3390/s17010208 Bogena, H. R., Montzka, C., Huisman, J. A., Graf, A., Schmidt, M., Stockinger, M., von Hebel, C., 715 716 Hendricks-Franssen, H. J., van der Kruk, J., Tappe, W., Lücke, A., Baatz, R., Bol, R., Groh, J., 717 Pütz, T., Jakobi, J., Kunkel, R., Sorg, J., & Vereecken, H. (2018). The TERENO-Rur 718 Hydrological Observatory: A Multiscale Multi-Compartment Research Platform for the 719 Advancement of Hydrological Science. Vadose Zone Journal, 17(1), 1–22. 720 https://doi.org/10.2136/vzj2018.03.0055 721 Borchardt, H. (2012). Einfluss periglazialer Deckschichten auf Abflusssteuerung am Beispiel des 722 anthropogen überprägten Wüstebaches. Rheinisch-Westfälische Technische Hochschule 723 Aachen. 724 Brocca, L., Tullo, T., Melone, F., Moramarco, T., & Morbidelli, R. (2012). Catchment scale soil 725 moisture spatial-temporal variability. *Journal of Hydrology*, 422–423, 63–75. 726 https://doi.org/10.1016/j.jhydrol.2011.12.039 727 Brutsaert, W., & Nieber, J. L. (1977). Regionalized drought flow hydrographs from a mature glaciated 728 plateau. Water Resources Research, 13(3), 637-643. 729 Chen, B., & Krajewski, W. (2016). Analysing individual recession events: sensitivity of parameter determination to the calculation procedure. Hydrological Sciences Journal, 61(16), 2887–2901. 730 731 https://doi.org/10.1080/02626667.2016.1170940 732 Chen, X., Parajka, J., Széles, B., Strauss, P., & Blöschl, G. (2020a). Controls on event runoff 733 coefficients and recession coefficients for different runoff generation mechanisms identified by 734 three regression methods. Journal of Hydrology and Hydromechanics, 68(2), 155–169. 735 https://doi.org/10.2478/johh-2020-0008

of event runoff characteristics in a small agricultural catchment. Hydrological Sciences Journal,

Chen, X., Parajka, J., Széles, B., Strauss, P., & Blöschl, G. (2020b). Spatial and temporal variability

736

- 738 65(13), 2185–2195. https://doi.org/10.1080/02626667.2020.1798451
- 739 Detty, J. M., & McGuire, K. J. (2010). Threshold changes in storm runoff generation at a till-mantled
- headwater catchment. Water Resources Research, 46(7), 1–15.
- 741 https://doi.org/10.1029/2009WR008102
- 742 Dralle, D. N., Karst, N., Charalampous, K., Veenstra, A., & Thompson, S. E. (2017). Event-scale
- power law recession analysis: Quantifying methodological uncertainty. *Hydrology and Earth*
- 744 System Sciences, 21(1), 65–81. https://doi.org/10.5194/hess-21-65-2017
- 745 Dralle, D. N., Karst, N., & Thompson, S. E. (2015). A, b careful: The challenge of scale invariance
- for comparative analyses in power law models of the streamflow recession. *Geophysical*
- 747 Research Letters, 42(21), 9285–9293. https://doi.org/10.1002/2015GL066007
- Eder, A., Weigelhofer, G., Pucher, M., Tiefenbacher, A., Strauss, P., Brandl, M., & Blöschl, G.
- 749 (2022). Pathways and composition of dissolved organic carbon in a small agricultural catchment
- during base flow conditions. *Ecohydrology and Hydrobiology*, 22(1), 96–112.
- 751 https://doi.org/10.1016/j.ecohyd.2021.07.012
- Exner-Kittridge, M., Strauss, P., Blöschl, G., Eder, A., Saracevic, E., & Zessner, M. (2016). The
- 753 seasonal dynamics of the stream sources and input flow paths of water and nitrogen of an
- Austrian headwater agricultural catchment. *Science of the Total Environment*, 542, 935–945.
- 755 https://doi.org/10.1016/j.scitotenv.2015.10.151
- Gaál, L., Szolgay, J., Bacigál, T., Kohnová, S., Hlavčová, K., Výleta, R., Parajka, J., & Blöschl, G.
- 757 (2016). Similarity of empirical copulas of flood peak-volume relationships: A regional case
- 758 study of North-West Austria. Contributions to Geophysics and Geodesy, 46(3), 155–178.
- 759 https://doi.org/10.1515/congeo-2016-0011
- 760 Gaál, L., Szolgay, J., Kohnová, S., Hlavčová, K., Parajka, J., Viglione, A., Merz, R., & Blöschl, G.
- 761 (2015). Dependence between flood peaks and volumes: a case study on climate and hydrological
- 762 controls. *Hydrological Sciences Journal*, 60(6), 968–984.

- 763 https://doi.org/10.1080/02626667.2014.951361 Gaál, L., Szolgay, J., Kohnová, S., Parajka, J., Merz, R., Viglione, A., & Blöschl, G. (2012). Flood 764 765 timescales: Understanding the interplay of climate and catchment processes through comparative 766 hydrology. Water Resources Research, 48(4). https://doi.org/10.1029/2011WR011509 767 Gebler, S., Kurtz, W., Pauwels, V. R. N., Kollet, S. J., Vereecken, H., & Hendricks Franssen, H. J. 768 (2019). Assimilation of High-Resolution Soil Moisture Data Into an Integrated Terrestrial Model 769 for a Small-Scale Head-Water Catchment. Water Resources Research, 55(12), 10358–10385. 770 https://doi.org/10.1029/2018WR024658 771 Giani, G., Tarasova, L., Woods, R. A., & Rico-Ramirez, M. A. (2022). An Objective Time-Series-772 Analysis Method for Rainfall-Runoff Event Identification. Water Resources Research, 58(2). 773 https://doi.org/10.1029/2021WR031283 774 Graf, A., Bogena, H. R., Drüe, C., Hardelauf, H., Pütz, T., Heinemann, G., & Vereecken, H. (2014). 775 Spatiotemporal relations between water budget components and soil water content in a forested 776 tributary catchment. Water Resources Research, 50(6), 4837–4857. 777 https://doi.org/10.1002/2013WR014516 Grimaldi, C., Thomas, Z., Fossey, M., Fauvel, Y., & Merot, P. (2009). High chloride concentrations 778 779 in the soil and groundwater under an oak hedge in the West of France: an indicator of 780 evapotranspiration and water movement. *Hydrological Processes*, 23, 1865–1873. 781 https://doi.org/10.1002/hyp.7316 782 Guo, D., Westra, S., & Maier, H. R. (2017a). Impact of evapotranspiration process representation on
- Guo, D., Westra, S., & Maier, H. R. (2017b). Use of a scenario-neutral approach to identify the key hydro-meteorological attributes that impact runoff from a natural catchment. *Journal of Hydrology*, 554, 317–330. https://doi.org/10.1016/j.jhydrol.2017.09.021

435–454. https://doi.org/10.1002/2016WR019627

783

784

runoff projections from conceptual rainfall-runoff models. Water Resources Research, 53(1),

- Harman, C. J., Sivapalan, M., & Kumar, P. (2009). Power law catchment-scale recessions arising
- from heterogeneous linear small-scale dynamics. Water Resources Research, 45(9), 1–13.
- 790 https://doi.org/10.1029/2008WR007392
- Hövel, A., Stumpp, C., Bogena, H., Lücke, A., Strauss, P., Blöschl, G., & Stockinger, M. (2024a).
- Repeating patterns in runoff time series: A basis for exploring hydrologic similarity of
- 793 precipitation and catchment wetness conditions. *Journal of Hydrology*, 629.
- 794 https://doi.org/10.1016/j.jhydrol.2023.130585
- Hövel, A., Stumpp, C., Bogena, H., Lücke, A., Strauss, P., Blöschl, G., & Stockinger, M. (2024b).
- Supplement to "Hydro-Meteorological Drivers of Event Runoff Characteristics Under Similar
- 797 Soil Moisture Patterns in Three Small-Scale Headwater Catchments" [Data set]. Zenodo.
- 798 https://doi.org/10.5281/zenodo.13753239
- Hrachowitz, M., Savenije, H. H. G., Blöschl, G., McDonnell, J. J., Sivapalan, M., Pomeroy, J. W.,
- Arheimer, B., Blume, T., Clark, M. P., Ehret, U., Fenicia, F., Freer, J. E., Gelfan, A., Gupta, H.
- V., Hughes, D. A., Hut, R. W., Montanari, A., Pande, S., Tetzlaff, D., ... Cudennec, C. (2013).
- A decade of Predictions in Ungauged Basins (PUB)-a review. *Hydrological Sciences Journal*,
- 803 58(6), 1198–1255. https://doi.org/10.1080/02626667.2013.803183
- Hrachowitz, M., Stockinger, M., Coenders-Gerrits, M., Van Der Ent, R., Bogena, H., Lücke, A., &
- Stumpp, C. (2021). Reduction of vegetation-accessible water storage capacity after deforestation
- affects catchment travel time distributions and increases young water fractions in a headwater
- catchment. *Hydrology and Earth System Sciences*, 25(9), 4887–4915.
- 808 https://doi.org/10.5194/hess-25-4887-2021
- James, A. L., & Roulet, N. T. (2007). Investigating hydrologic connectivity and its association with
- threshold change in runoff response in a temperate forested watershed. *Hydrological Processes*,
- 811 21, 3391–3408. https://doi.org/10.1002/hyp.6554
- Jencso, K. G., & McGlynn, B. L. (2011). Hierarchical controls on runoff generation: Topographically
- driven hydrologic connectivity, geology, and vegetation. Water Resources Research, 47(11), 1–

314	16. https://doi.org/10.1029/2011WR010666
315	Jencso, K. G., McGlynn, B. L., Gooseff, M. N., Wondzell, S. M., Bencala, K. E., & Marshall, L. A.
816	(2009). Hydrologic connectivity between landscapes and streams: Transferring reach- and plot-
817	scale understanding to the catchment scale. Water Resources Research, 45(4), 1–16.
818	https://doi.org/10.1029/2008WR007225
819	Kirchner, J. W. (2024). Characterizing nonlinear, nonstationary, and heterogeneous hydrologic
820	behavior using Ensemble Rainfall-Runoff Analysis (ERRA): proof of concept. Hydrology and
321	Earth System Sciences, 28, 4427-4454. https://doi.org/10.5194/hess-28-4427-2024
322	Korres, W., Reichenau, T. G., Fiener, P., Koyama, C. N., Bogena, H. R., Cornelissen, T., Baatz, R.,
323	Herbst, M., Diekkrüger, B., Vereecken, H., & Schneider, K. (2015). Spatio-temporal soil
324	moisture patterns - A meta-analysis using plot to catchment scale data. Journal of Hydrology,
325	520, 326–341. https://doi.org/10.1016/j.jhydrol.2014.11.042
826	Latron, J., & Gallart, F. (2008). Runoff generation processes in a small Mediterranean research
327	catchment (Vallcebre, Eastern Pyrenees). Journal of Hydrology, 358(3-4), 206-220.
828	https://doi.org/10.1016/j.jhydrol.2008.06.014
829	Lee, J. Y., Yang, C. J., Peng, T. R., Lee, T. Y., & Huang, J. C. (2023). Landscape structures regulate
830	the contrasting response of recession along rainfall amounts. Hydrology and Earth System
331	Sciences, 27(23), 4279–4294. https://doi.org/10.5194/hess-27-4279-2023
332	Li, Y. Y., & Shao, M. A. (2006). Change of soil physical properties under long-term natural
333	vegetation restoration in the Loess Plateau of China. Journal of Arid Environments, 64(1), 77-
334	96. https://doi.org/10.1016/j.jaridenv.2005.04.005
335	Lindström, G. (1997). A simple automatic calibration routine for the HBV model. 28(3), 153–168.
836	Liu, S., Van Meerveld, I., Zhao, Y., Wang, Y., & Kirchner, J. W. (2024). Seasonal dynamics and
337	spatial patterns of soil moisture in a loess catchment. Hydrology and Earth System Sciences,
338	28(1), 205–216, https://doi.org/10.5194/hess-28-205-2024

839 Madrid, F., Imani, S., Mercer, R., Zimmerman, Z., Shakibay, N., & Keogh, E. (2019). Matrix profile 840 XX: Finding and visualizing time series motifs of all lengths using the matrix profile. 841 Proceedings - 10th IEEE International Conference on Big Knowledge, ICBK 2019, 175–182. https://doi.org/10.1109/ICBK.2019.00031 842 843 Mälicke, M., Hassler, S. K., Blume, T., Weiler, M., & Zehe, E. (2020). Soil moisture: Variable in 844 space but redundant in time. Hydrology and Earth System Sciences, 24(5), 2633–2653. https://doi.org/10.5194/hess-24-2633-2020 845 McDonnell, J. J. (2013). Are all runoff processes the same? Hydrological Processes, 27(26), 4103-846 847 4111. https://doi.org/10.1002/hyp.10076 848 McGrath, G. S., Hinz, C., & Sivapalan, M. (2007). Temporal dynamics of hydrological threshold 849 events. Hydrology and Earth System Sciences, 11(2), 923-938. https://doi.org/10.5194/hess-11-923-2007 850 851 Merz, R., & Blöschl, G. (2009). A regional analysis of event runoff coefficients with respect to 852 climate and catchment characteristics in Austria. Water Resources Research, 45(1), 1–19. https://doi.org/10.1029/2008WR007163 853 854 Merz, R., Blöschl, G., & Parajka, J. (2006). Spatio-temporal variability of event runoff coefficients. Journal of Hydrology, 331(3-4), 591-604. https://doi.org/10.1016/j.jhydrol.2006.06.008 855 856 Mohanty, B. P., Cosh, M. H., Lakshmi, V., & Montzka, C. (2017). Soil Moisture Remote Sensing: 857 State-of-the-Science. Vadose Zone Journal, 16(1), 1–9. https://doi.org/10.2136/vzj2016.10.0105 858 Moriasi, D. N., Arnold, J. G., Liew, M. W. Van, Bingner, R. L., Harmel, R. D., & Veith, T. L. (2007). 859 Model evaluation guidelines for systematic quantification of accuracy in watershed simulations. 860 *Transactions of the ASABE*, 50(3), 885–900. Parajka, J., Blöschl, G., & Merz, R. (2007). Regional calibration of catchment models: Potential for 861 ungauged catchments. Water Resources Research, 43(6), 1–16. 862 https://doi.org/10.1029/2006WR005271 863

Patnaik, S., Biswal, B., Nagesh Kumar, D., & Sivakumar, B. (2015). Effect of catchment 864 865 characteristics on the relationship between past discharge and the power law recession coefficient. Journal of Hydrology, 528, 321–328. https://doi.org/10.1016/j.jhydrol.2015.06.032 866 867 Pavlin, L., Széles, B., Strauss, P., Blaschke, A. P., & Blöschl, G. (2021). Event and seasonal 868 hydrologic connectivity patterns in an agricultural headwater catchment. Hydrology and Earth 869 System Sciences, 25(4), 2327–2352. https://doi.org/10.5194/hess-25-2327-2021 Penna, D., Tromp-Van Meerveld, H. J., Gobbi, A., Borga, M., & Dalla Fontana, G. (2011). The 870 871 influence of soil moisture on threshold runoff generation processes in an alpine headwater 872 catchment. Hydrology and Earth System Sciences, 15(3), 689-702. https://doi.org/10.5194/hess-15-689-2011 873 874 Qu, W., Bogena, H. R., Huisman, J. A., Schmidt, M., Kunkel, R., Weuthen, A., Schiedung, H., Schilling, B., Sorg, J., & Vereecken, H. (2016). The integrated water balance and soil data set of 875 876 the Rollesbroich hydrological observatory. Earth System Science Data, 8(2), 517–529. 877 https://doi.org/10.5194/essd-8-517-2016 878 Qu, W., Bogena, H. R., Huisman, J. A., & Vereecken, H. (2013). Calibration of a novel low-cost soil 879 water content sensor based on a ring oscillator. Vadose Zone Journal, 12(2), 1-10. https://doi.org/10.2136/vzj2012.0139 880 881 Richter, F. (2008). Bodenkarte zur Standorterkundung. Verfahren Quellgebiet Wüstebachtal (Forst). 882 Geologischer Dienst Nordrhein-Westfalen, Krefeld, Germany. 883 Rosenbaum, U., Bogena, H. R., Herbst, M., Huisman, J. A., Peterson, T. J., Weuthen, A., Western, A. 884 W., & Vereecken, H. (2012). Seasonal and event dynamics of spatial soil moisture patterns at the small catchment scale. Water Resources Research, 48(10), 1–22. 885 886 https://doi.org/10.1029/2011WR011518 887 Ross, C. A., Ali, G., Spence, C., Oswald, C., & Casson, N. (2019). Comparison of event-specific 888 rainfall-runoff responses and their controls in contrasting geographic areas. Hydrological

889 Processes, 33(14), 1961–1979. https://doi.org/10.1002/hyp.13460 890 Rossi, M. W., Whipple, K. X., & Vivoni, E. R. (2016). Precipitation and evapotranspiration controls 891 on daily runoff variability. Journal of Geophysical Research: Earth Surface, 121(1), 128–145. 892 https://doi.org/10.1002/2015JF003446 893 Saffarpour, S., Western, A. W., Adams, R., & McDonnell, J. J. (2016). Multiple runoff processes and 894 multiple thresholds control agricultural runoff generation. Hydrology and Earth System 895 Sciences, 20(11), 4525–4545. https://doi.org/10.5194/hess-20-4525-2016 896 Saleh, A., Arnold, J. G., Gassman, P. W., Hauck, L. M., Rosenthal, W. D., Williams, J. R., & 897 McFarland, A. M. S. (2000). Application of SWAT for the Upper North Bosque River 898 Watershed. Transactions of the American Society of Agricultural Engineers, 43(5), 1077–1087. 899 https://doi.org/10.13031/2013.3000 900 Sherman, L. (1932). Streamflow from rainfall by the unit-graph method. Engineering News Records, 901 *108*, 501–505. 902 Singh, J., Knapp, H. V., Arnold, J. G., & Demissie, M. (2005). Hydrological modeling of the Iroquois 903 River watershed using HSPF and SWAT. Journal of the American Water Resources Association, 41(2), 343–360. https://doi.org/10.1111/j.1752-1688.2005.tb03740.x 904 905 Singh, N. K., Emanuel, R. E., McGlynn, B. L., & Miniat, C. F. (2021). Soil Moisture Responses to 906 Rainfall: Implications for Runoff Generation. Water Resources Research, 57(9), 1–17. 907 https://doi.org/10.1029/2020WR028827 908 Stein, L., Pianosi, F., & Woods, R. (2020). Event-based classification for global study of river flood 909 generating processes. *Hydrological Processes*, 34(7), 1514–1529. 910 https://doi.org/10.1002/hyp.13678 911 Stockinger, M., Bogena, H. R., Lücke, A., Diekkrüger, B., Weiler, M., & Vereecken, H. (2014). 912 Seasonal soil moisture patterns: Controlling transit time distributions in a forested headwater catchment. Water Resources Research, 50(6), 5270-5289. 913

914	https://doi.org/10.1002/2013WR014815
915	Stockinger, M., Bogena, H. R., Lücke, A., Stumpp, C., & Vereecken, H. (2019). Time variability and
916	uncertainty in the fraction of young water in a small headwater catchment. Hydrology and Earth
917	System Sciences, 23(10), 4333-4347. https://doi.org/10.5194/hess-23-4333-2019
918	Széles, B., Broer, M., Parajka, J., Hogan, P., Eder, A., Strauss, P., & Blöschl, G. (2018). Separation of
919	Scales in Transpiration Effects on Low Flows: A Spatial Analysis in the Hydrological Open Air
920	Laboratory. Water Resources Research, 54(9), 6168-6188.
921	https://doi.org/10.1029/2017WR022037
922	Szeles, B., Holko, L., Parajka, J., Stumpp, C., Stockinger, M., Komma, J., Rab, G., Wyhlidal, S.,
923	Schott, K., Hogan, P., Pavlin, L., Strauss, P., Schmaltz, E., & Blöschl, G. (2024). Comparison of
924	two isotopic hydrograph separation methods in the Hydrological Open Air Laboratory, Austria.
925	Hydrological Processes, 38(7), 1–15. https://doi.org/10.1002/hyp.15222
926	Tarasova, L., Basso, S., Poncelet, C., & Merz, R. (2018a). Exploring Controls on Rainfall-Runoff
927	Events: 2. Regional Patterns and Spatial Controls of Event Characteristics in Germany. Water
928	Resources Research, 54(10), 7688–7710. https://doi.org/10.1029/2018WR022588
929	Tarasova, L., Basso, S., Zink, M., & Merz, R. (2018b). Exploring Controls on Rainfall-Runoff
930	Events: 1. Time Series-Based Event Separation and Temporal Dynamics of Event Runoff
931	Response in Germany. Water Resources Research, 54(10), 7711–7732.
932	https://doi.org/10.1029/2018WR022587
933	TERENO (2024). TERENO Data Discovery Portal - Eifel/Lower Rhine Valley Observatory.
934	https://ddp.tereno.net/ddp/
935	Tromp-Van Meerveld, H. J., & McDonnell, J. J. (2006). Threshold relations in subsurface stormflow:
936	2. The fill and spill hypothesis. Water Resources Research, 42(2), 1–11.
937	https://doi.org/10.1029/2004WR003800
938	Vichta, T., Deutscher, J., Hemr, O., Tomášová, G., Žižlavská, N., Brychtová, M., Bajer, A., & Shukla,

939 M. K. (2024). Combined effects of rainfall-runoff events and antecedent soil moisture on runoff 940 generation processes in an upland forested headwater area. Hydrological Processes, 38(6), 1–15. 941 https://doi.org/10.1002/hyp.15216 942 Vreugdenhil, M., Széles, B., Wagner, W., Strauß, P., Oismueller, M., Parajka, J., Blöschl, G., & 943 Hogan, P. (2022). Non-linearity in event runoff generation in a small agricultural catchment. 944 Hydrological Processes, 36(8), 1–16. https://doi.org/10.1002/hyp.14667 Wiekenkamp, I., Huisman, J. A., Bogena, H. R., Graf, A., Lin, H. S., Drüe, C., & Vereecken, H. 945 946 (2016a). Changes in measured spatiotemporal patterns of hydrological response after partial 947 deforestation in a headwater catchment. Journal of Hydrology, 542, 648–661. 948 https://doi.org/10.1016/j.jhydrol.2016.09.037 949 Wiekenkamp, I., Huisman, J. A., Bogena, H. R., Lin, H. S., & Vereecken, H. (2016b). Spatial and 950 temporal occurrence of preferential flow in a forested headwater catchment. Journal of 951 *Hydrology*, *534*, 139–149. https://doi.org/10.1016/j.jhydrol.2015.12.050 952 Wittenberg, H., & Sivapalan, M. (1999). Watershed groundwater balance estimation using streamflow 953 recession analysis and baseflow separation. Journal of Hydrology, 219(1-2), 20-33. https://doi.org/10.1016/S0022-1694(99)00040-2 954 955 Yao, L., Libera, D. A., Kheimi, M., Sankarasubramanian, A., & Wang, D. (2020). The Roles of 956 Climate Forcing and Its Variability on Streamflow at Daily, Monthly, Annual, and Long-Term 957 Scales. Water Resources Research, 55(7), 1–23. https://doi.org/10.1029/2020WR027111 958 Yeh, C.-C. M., Zhu, Y., Ulanova, L., Begum, N., Ding, Y., Dau, H. A., Silva, D. F., Mueen, A., & 959 Keogh, E. (2016). Matrix Profile I: All Pairs Similarity Joins for Time Series: A Unifying View 960 That Includes Motifs, Discords and Shapelets. IEEE 16th International Conference on Data 961 Mining (ICDM), 1317–1322. https://doi.org/10.1109/icdm.2016.0179 962 Zacharias, S., Bogena, H., Samaniego, L., Mauder, M., Fuß, R., Pütz, T., Frenzel, M., Schwank, M., Baessler, C., Butterbach-Bahl, K., Bens, O., Borg, E., Brauer, A., Dietrich, P., Hajnsek, I., Helle, 963

964	G., Kiese, R., Kunstmann, H., Klotz, S., Vereecken, H. (2011). A Network of Terrestrial
965	Environmental Observatories in Germany. Vadose Zone Journal, 10(3), 955-973.
966	https://doi.org/10.2136/vzj2010.0139
967	Zehe, E., Elsenbeer, H., Lindenmaier, F., Schulz, K., & Blöschl, G. (2007). Patterns of predictability
968	in hydrological threshold systems. Water Resources Research, 43(7), 1–12.
969	https://doi.org/10.1029/2006WR005589
970	Zheng, Y., Coxon, G., Woods, R., Li, J., & Feng, P. (2023). Controls on the Spatial and Temporal
971	Patterns of Rainfall-Runoff Event Characteristics – A Large Sample of Catchments Across Great
972	Britain. Water Resources Research, 59(6). https://doi.org/10.1029/2022wr033226